Marrow Toxicity of ^{33}P- Versus ^{32}P-Orthophosphate: Implications for Therapy of Bone Pain and Bone Metastases

S. Murty Goddu, Anupam Bishayee, Lionel G. Bouchet, Wesley E. Bolch, Dandamudi V. Rao, and Roger W. Howell

Department of Radiology, University of Medicine and Dentistry of New Jersey, New Jersey Medical School, Newark, New Jersey; and Department of Nuclear and Radiological Engineering, University of Florida, Gainesville, Florida

Several bone-seeking radiopharmaceuticals, such as ^{32}P-orthophosphate, ^{89}Sr-chloride, ^{186}Re-1,1 hydroxyethylidene diphosphonate (HEDP), and ^{153}Sm-ethylene diamine tetramethylene phosphonic acid (EDTMP), have been used to treat bone pain. The major limiting factor with this modality is bone marrow toxicity, which arises from the penetrating nature of the high-energy β particles emitted by the radionuclides. It has been hypothesized that marrow toxicity can be reduced while maintaining therapeutic efficacy by using radionuclides that emit short-range β particles or conversion electrons. In view of the significant clinical experience with ^{32}P-orthophosphate, and the similarity in pain relief afforded by ^{32}P-orthophosphate and ^{89}Sr-chloride, this hypothesis is examined in this study using ^{32}P- and ^{33}P-orthophosphate in a mouse femur model. **Methods:** Survival of granulocyte macrophage colony-forming cells (GM-CFCs) in femoral marrow was used as a biologic dosimeter for bone marrow. ^{32}P- and ^{33}P-orthophosphate were administered intravenously, and GM-CFC survival was determined as a function of time after injection and, at the nadir, as a function of injected activity. The kinetics of radioactivity in the marrow, muscle, and femoral bone were also determined. The biologic dosimeter was calibrated by assessing GM-CFC survival at its nadir after chronic irradiation of Swiss Webster mice with exponentially decreasing dose rates of γ rays (relative biologic effectiveness equivalent to that of β particles) from a low-dose rate ^{137}Cs irradiator. Dose-rate decrease half-times (T_d) (time required for ^{137}Cs γ ray dose rate to decrease by one half) of 62, 255, and 425 h and infinity were used to simulate the dose rate patterns delivered by the radiopharmaceuticals as dictated by their effective clearance half-times from the mouse femurs. These data were used to experimentally determine the mean absorbed dose to the femoral marrow per unit injected activity. Finally, a theoretical dosimetry model of the mouse femur was developed, and the absorbed doses to the femoral marrow, bone, and endosteum were calculated using the EGS4 Monte Carlo code. **Results:** When the animals were irradiated with exponentially decreasing dose rates of ^{137}Cs γ rays, initial dose rates required to achieve 37% survival were 1.9, 0.98, 0.88, and 0.79 cGy/h for dose rate decrease half-times of 62, 255, and 425 h and infinity, respectively. The D_{37} values were 144 ± 15, 132 ± 12, 129 ± 3, and 133 ± 10 cGy, respectively, compared with a value of 103 cGy for acute irradiation. When ^{32}P and ^{33}P were administered, the injected activities required to achieve 37% survival were 313 and 2820 kBq, respectively. Theoretical dosimetry calculations show that ^{33}P offers a 3- to 6-fold therapeutic advantage over ^{32}P, depending on the source and target regions assumed. **Conclusion:** The low-energy β-particle emitter ^{33}P appears to offer a substantial dosimetric advantage over energetic β-particle emitters (e.g., ^{32}P, ^{89}Sr, ^{186}Re) for irradiating bone and minimizing marrow toxicity. This suggests that low-energy β or conversion electron emitters may offer a substantial advantage for alleviation of bone pain as well as for specifically irradiating metastatic disease in bone.

Key Words: bone; pain; metastases; radionuclides; granulocyte macrophage colony-forming cells; chronic irradiation; dose response; dosimetry; EGS4; ^{32}P; ^{33}P therapy

J Nucl Med 2000; 41:941–951

Over the past 50 y several bone-seeking radiopharmaceuticals have been used to treat bone pain caused by osteometastases (*1,2*). The response rate for most radiopharmaceuticals used to alleviate bone pain varies from 65% to 85% (*3*). Radioactive phosphorus (^{32}P) was the first (*4*) and at one time the most widely used radionuclide in bone pain palliation therapy (*1*). More recently, other radiopharmaceuticals, including ^{89}Sr-chloride (*2,5*), ^{186}Re-1,1 hydroxyethylidene diphosphonate (HEDP) (*6,7*), and ^{153}Sm-ethylene diamine tetramethylene phosphonic acid (EDTMP) (*8,9*) have been used for this purpose.

The major dose-limiting factor with this modality is bone marrow toxicity, which results in a reduction of peripheral blood cell counts (*1,10*). The absorbed dose to the bone marrow from internal radionuclides can come from 4 principal sources: (a) activity within the marrow compartment, (b) activity in the endosteal region, (c) activity in the bone matrix, and (d) activity in all other surrounding organs. Because most of the radiopharmaceuticals used in bone palliation therapy localize predominantly in the skeletal tissues and emit high-energy β particles, the marrow absorbed dose comes mainly from the first 3 components. In fact, these radiopharmaceuticals selectively localize in bone

and concentrate in the bony lesions with very little activity localizing in the marrow compartment (2,11). Therefore, the bone marrow toxicity arises mainly from the second and third components because of the penetrating nature of the high-energy β particles emitted by these radionuclides. It has been suggested that use of low-energy electron emitters (e.g., short-range) might reduce the bone marrow toxicity and selectively increase the dose to the bone matrix (12,13). Atkins et al. (14) used the low-energy conversion electron emitter [117m]Sn-labeled diethylenetriamine pentaacetic acid ([117m]Sn(4+)DTPA) to treat bone pain in several patients and found effective pain relief with reduced bone marrow toxicity. This reduction in bone marrow toxicity was realized despite localization of the [117m]Sn at the actively mineralizing osteoid surface, which is in close proximity to the marrow (15).

In view of the potential marrow-sparing capacity of low-energy electron emitters, this study was undertaken to examine the dosimetry characteristics of the low-energy β-emitter [33]P [mean energy, 77 keV; mean range in bone, ~60 μm (16)] versus the high energy β-emitter [32]P (mean energy, 695 keV; mean range in bone, ~1.7 mm). The low-energy ^{33}P was suggested as a good candidate for this modality by Tofe et al. (13) and Potsaid et al. (12). However, to the best of our knowledge, this approach was never clinically pursued. In this study, the capacity of ^{33}P-orthophosphate to irradiate the bone matrix and endosteum while minimizing the absorbed dose to bone marrow is compared with the high-energy β-particle emitting radiopharmaceutical ^{32}P-orthophosphate. A combination of experimental and theoretical approaches based on a Swiss Webster mouse model are used to make this comparison. Femoral bone marrow granulocyte-macrophage colony-forming cell (GM-CFC) survival is used to experimentally ascertain bone marrow toxicity and absorbed dose from these radionuclides after intravenous administration (17,18). A theoretical approach was developed to calculate the absorbed dose delivered to the bone matrix. These results are used to make a dosimetric comparison between ^{33}P and ^{32}P for palliation of bone pain.

MATERIALS AND METHODS

Biologic Dosimetry Using GM-CFC Survival

GM-CFC survival was used as a biologic dosimeter to determine the bone marrow absorbed dose in mice. GM-CFCs are progenitor cells that reside in the marrow compartment. Therefore, the absorbed dose received by the bone marrow can be determined by monitoring the survival of these cells, provided the system is properly calibrated. Details on the use of GM-CFC as a biologic dosimeter have been described previously (18).

Animals

Female Swiss-Webster mice (5–6 wk old; weight, 25 ± 2 g) were obtained from Taconic Farms (Germantown, NY). The animals were acclimated in the University Research Animal Facility for 1 wk before use. Food and water were provided ad libitum. All procedures were approved by the University Institu-

tional Animal Care and Use Committee, University of Medicine and Dentistry of New Jersey (Newark, NJ).

Radionuclides and Administration

Carrier-free ^{32}P and ^{33}P were obtained from DuPont NEN Research Products (Boston, MA) as orthophosphoric acid in 1 mL water. These radiopharmaceuticals were buffered with equal amounts of double-strength phosphate-buffered saline (PBS) and diluted in large quantities of regular strength PBS. Mice, in groups of 4, were injected intravenously through the tail vein with 200 μL solution containing the radiopharmaceutical.

Radionuclide Kinetics and Optimal Day for GM-CFC Survival Assay

The biokinetics and the optimal assay day for the GM-CFC survival assay were determined simultaneously for ^{32}P-orthophosphoric acid. Ten groups of 4 animals each were injected intravenously with equal amounts of radiopharmaceutical on days 1, 2, 3, 4, 6, 7, 9, 10, 15, and 23 before the date of kill. An additional 2 untouched groups were maintained as controls. Experiments were performed for 2 different injection activities (14.8 and 29.6 kBq/g of body weight) to ensure that injected activity did not influence the kinetics. All groups were killed on the same day and assayed for GM-CFC survival, and the survival fraction compared with controls was plotted as a function of time after injection. Aliquots of the bone marrow, which was flushed from the femurs for the GM-CFC assay, were added to a liquid scintillation cocktail and counted in a Beckman LS3800 liquid scintillation counter ([LSC]; Beckman, Fullerton, CA) to a statistical uncertainty of less than 1%. The flushed femurs were dried and transferred to preweighed scintillation vials. The muscle surrounding the femur was also removed and transferred to preweighed scintillation vials. Sample weights were determined and the vials were subsequently counted for Cerenkov radiation (18). The activities in muscle, bone matrix, and marrow compartments were thus determined as functions of time after injection.

To determine ^{33}P kinetics, 40 mice were injected intravenously with ^{33}P-orthophosphate (3.7 kBq/g body weight). At different times after administration, the animals were killed in groups of 4 and the femurs were flushed of marrow and transferred to preweighed 20-mL glass scintillation vials. On measuring the sample weights, 4 mL decalcifying solution (Poly Scientific Research and Development Corp., Bayshore, NY) were added to each vial and placed on an orbital shaker at 40°C for 3 d. Then, 15 mL Aquasol liquid scintillation cocktail (DuPont NEN Research Products) were added, and the vial was counted in the Beckman LSC. To determine the counting efficiency, femurs from control mice were dissolved similarly in 4 mL decalcifying solution, and 15 mL Aquasol along with a known amount of ^{33}P were added. The counting efficiency was found to be 100%. To obtain the activity in the bone marrow, aliquots of the marrow solution were mixed with Aquasol and the activity determined using the Beckman LSC. Muscle kinetics were not directly measured for ^{33}P, because, in this case, muscle activity does not significantly contribute to the marrow or bone dose. Therefore, the muscle kinetics for ^{33}P-orthophosphate were determined by first calculating the biologic clearance half-time (T_b) of ^{32}P-orthophosphate in muscle ($T_b = T_e(^{32}P)T_p(^{32}P)/[T_p(^{32}P) - T_e(^{32}P)]$). Assuming the biologic half-times are equal, the effective half-time of ^{33}P in muscle is given by $T_e(^{33}P) = T_bT_p(^{33}P)/(T_p(^{33}P) + T_b)$.

Culture Media for GM-CFC Survival Assay

The wash medium contained 13.37 g Dulbecco's modified Eagle's medium HG powder (DMEM), 984 mL distilled/deionized water, 4 mL L-asparagine (20 μg/mL), 2 mL DEAE dextran (75 μg/mL; Sigma Chemical Co., St. Louis, MO), 10 mL penstrep (5000 U/mL penicillin and 5000 μg/mL streptomycin), 3.7 g NaHCO₃, and 2% horse serum (19). However, for bone marrow cultures, double-strength culture medium with 60% horse serum was used. This was prepared by mixing 13.7 g DMEM in 484 mL distilled/deionized water, 4 mL L-asparagine (20 μg/mL), 2 mL DEAE dextran (75 μg/mL), 10 mL penstrep, 3.7 g NaHCO3, and 60% horse serum. All reagents, except as noted, were from GIBCO Laboratories (Grand Island, NY).

GM-CFC Survival Assay

The experimental protocols adopted from Metcalf (20) and described in an earlier article by this group (18) were used for determining GM-CFC survival. Briefly, the animals were killed, immersed in 70% ethanol, and the femurs were separated under aseptic conditions (laminar flow hood) using sterile instruments. Marrow from these femurs was flushed with 1 mL wash medium into a 50-mL tube using a 3-mL syringe fitted with a 21-gauge needle. After aspirating the medium through the femur shaft several times, an additional 3 mL fresh medium were flushed through the femur. The cell suspension was centrifuged, the supernatant decanted, and the pellet resuspended in 5 mL wash medium. The mononucleated cell fraction was separated from the crude bone marrow suspension by gently layering 5-mL cell suspension on top of 3.5-mL Histopaque-1077 (Sigma) and centrifuging at 400g for 30 min at 4°C. The mononucleated cell layer was removed carefully with a 3-mL syringe, washed 3 times with 15 mL wash medium, and resuspended in 2 mL double-strength culture medium. The viability of the cells was tested by trypan blue exclusion. More than 95% of cells were found to be viable. The number of mononucleated cells corresponding to each group was counted using a Coulter Model ZM cell counter (Coulter Electronics, Ltd., Hialeah, FL). Three dilutions of the resulting mononucleated cells were plated for colony formation by mixing with equal volumes of double-strength culture medium and 0.6% Bacto agar solution (dissolved in water and autoclaved) in the presence of 1200 U (20 μL) of recombinant murine granulocyte-macrophage colony stimulating factor (Sigma). The plates were allowed to stand at room temperature until the agar gelled firmly (10–15 min). They then were transferred to an incubator at 37°C with 100% humidity, 5% CO₂/95% air, for 7 d to allow for colony formation. The resulting GM-CFC colonies were scored with an Olympus dissection microscope (Olympus, Tokyo, Japan) at 40× magnification, and the survival fraction compared with unirradiated controls was determined.

GM-CFC Survival Versus Femoral Activity

GM-CFC survival was determined as a function of injected activity for both ³²P- and ³³P-orthophosphate. Six groups (4 per group) of mice were injected with a fixed 200-μL volume containing different activities of the radiopharmaceutical. The animals were killed on the optimal day (seventh day after injection) and assayed for GM-CFC survival. The femoral bones, having been purged of marrow for the survival assay, were dried, weighed, and assayed for activity content as described above. Activities in the flushed bone marrow samples were also determined. The extrapolated initial activities were obtained by correcting these activities to the time of injection, using the physical half-life of the radionu-

clides and the effective half-times of the radiopharmaceutical in the femurs obtained in the biokinetics experiments.

Calibration of the Biologic Dosimeter

The biologic dosimeter was calibrated using our custom-designed low-dose-rate ¹³⁷Cs irradiator (equipped with computer-controlled mercury attenuator system), which facilitates the delivery of exponentially decreasing dose rates (17). GM-CFC survival was used as a biologic dosimeter in these studies (18). This irradiator allows simultaneous irradiation of mice with different initial dose rates by placing different groups of mice at different distances from the ¹³⁷Cs source. Although the initial dose rates were different for each group of mice, the dose rates were exponentially decreased using a predetermined dose-rate decrease half-time (T_d), the time required for the dose rate to decrease by one-half. Mice, in groups of 4, were caged on different shelves in the irradiator cabinet, and the computer-driven mercury attenuator was programmed to deliver predefined initial dose rates to each cage and then decrease the dose rates with a fixed T_d. The dose rates and total doses to each cage were monitored during the irradiation period using Thomson-Nielsen MOSFET dosimeter probes customized for low-dose-rate measurements (Thomson & Nielsen Electronics, Ltd., Ottawa, Canada). Animals were taken out of the irradiator on the optimal day (seventh day after initiation of irradiation), killed, and assayed for GM-CFC cell survival. Three T_ds (62, 255, and 425 h) were used for these studies, and GM-CFC survival as a function of initial dose rate was obtained for each T_d. These T_ds correspond to the effective half-times of ⁹⁰Y-citrate (18), ³²P-orthophosphate, and ¹¹⁴ᵐIn-citrate in the femurs of the Swiss Webster mice (17). Similar experiments were also performed by irradiating mice with constant dose rates for 7 d and killing them on the same day. Again, the relationship between initial dose rate and GM-CFC survival was obtained.

Acute Irradiation

Animals were irradiated acutely in 2–5 min using a JL Shepherd Mark I irradiator (JL Shephard & Associates, San Fernando, CA) with dose rates ranging from 0.1 to 1 Gy/min and total irradiation times of 2–5 min. The animals were killed immediately after irradiation and assayed for GM-CFC survival.

Bone Measurements

After purging the marrow, low-pressure air was passed through the shaft using a 5-mL syringe. The femurs were transferred to preweighed borosilicate tubes and dried overnight. The femurs were reweighed and the bone mass determined. The marrow mass was determined by measuring the femur weights before and after purging the marrow using the procedures given in an earlier study (18).

Gross Activity Distribution in the Femur

The activity per gram femur was determined along the length of the femur. The femoral bones, having been purged of marrow for the survival assay, were sliced axially into about 5 sections, and each section was weighed and assayed for activity content as described above. The activity per gram remained essentially constant along the length of the femur.

RESULTS

Radionuclide Kinetics

The effective uptake and clearance of ³²P and ³³P in mouse femoral bone after intravenous administration of these radionuclides in the form of orthophosphate are shown in Figure 1. The rapid uptake and slow clearance patterns of ³²P
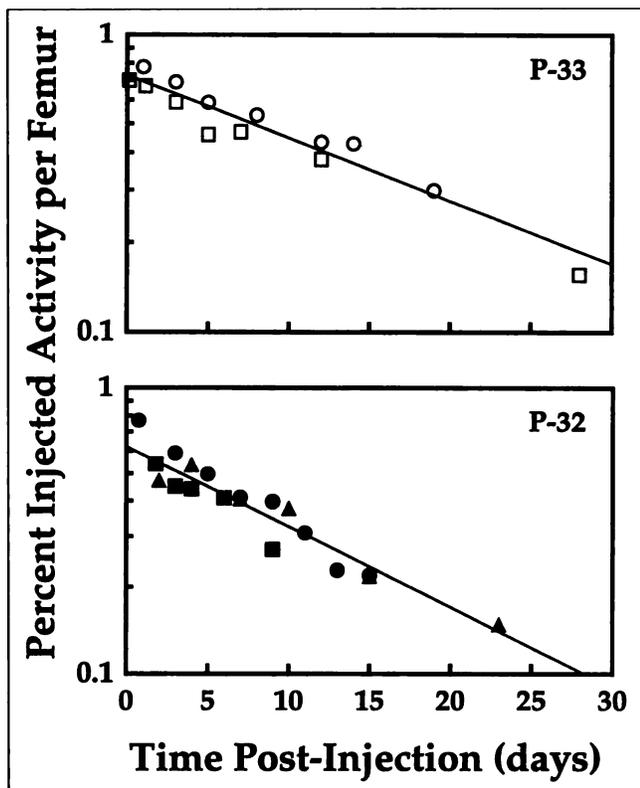
FIGURE 1. Effective clearance of radioactivity from mice femoral bone after intravenous administration of ^{32}P-orthophosphate (■, ▲, ●) and ^{33}P-orthophosphate (□, ○). Two independent experiments (denoted by different symbols) were performed for ^{33}P, and 3 were performed for ^{32}P. Results indicate that 0.67% of injected activity (of both ^{32}P and ^{33}P) quickly localizes in each femoral bone. ^{32}P-orthophosphate clears with effective half-time of 10.6 d, and ^{33}P-orthophosphate clears with 14.3 d half-time.

and ^{33}P were similar. A least-squares fit of the ^{32}P kinetics data to a single component exponential function yielded an effective half-time of 255 ± 38 h (10.6 ± 1.6 d). A similar fit to the ^{33}P data gave an effective half-time of 343 ± 38 h (14.3 ± 1.6 d). About 6% of the total femur activity was found in the marrow compartment, and its clearance followed essentially the same pattern as the bone. The uptake and clearance of ^{32}P was also determined in the muscle surrounding the femur and is shown in Figure 2. The uptake by muscle was very rapid and was followed by exponential clearance with an effective half-time of 226 ± 65 h (9.4 ± 2.7 d).

The extrapolated initial activity (A_o) in the femoral bone is plotted as a function of the injected activity (A_{Inj}) in Figure 3 for both ^{32}P and ^{33}P. In both cases, the extrapolated initial activity in the femoral bone was linearly dependent on the injected activity according to the relationship:

$$A_o = 0.0067 \, A_{Inj}. \qquad \text{Eq. 1}$$

These results indicate that 0.67% of the injected radioactive phosphorus (^{32}P and ^{33}P) localizes in femoral bone.

Optimal Day

The optimal day to assay GM-CFC survival is the day on which the survival is minimum (nadir). The survival of GM-CFC as a function of time after injection of a fixed activity of ^{32}P is shown in Figure 4. The survival fraction decreases rapidly, reaching a minimum on the seventh day after injection. This minimum is subsequently followed by a resurgence in the GM-CFC population as shown by the increasing survival fraction at longer times after injection.

GM-CFC Survival Versus Injected Activity

Figure 5 shows the GM-CFC survival fraction as a function of both the injected activity and extrapolated initial femoral bone activity after purging marrow for both ^{32}P and ^{33}P. The ^{32}P and ^{33}P data were fit by the least-squares technique to the following simple exponential relationships:

$$SF = \exp(-A_o/A_{o,37}) = \exp(-A_{Inj}/A_{Inj,37}), \qquad \text{Eq. 2}$$

where SF is the fraction of GM-CFC survival, A_o is the extrapolated initial femur activity, $A_{o,37}$ is the extrapolated initial femur activity required to achieve 37% GM-CFC survival, A_{Inj} is the total amount of activity injected into each mouse, and $A_{Inj,37}$ is the injected activity required to achieve 37% GM-CFC survival. The fitted values for $A_{o,37}$ were 2.1 kBq (0.056 µCi) and 18.9 kBq (0.51 µCi) per femur for ^{32}P and ^{33}P, respectively (Table 1). The fitted values for $A_{Inj,37}$
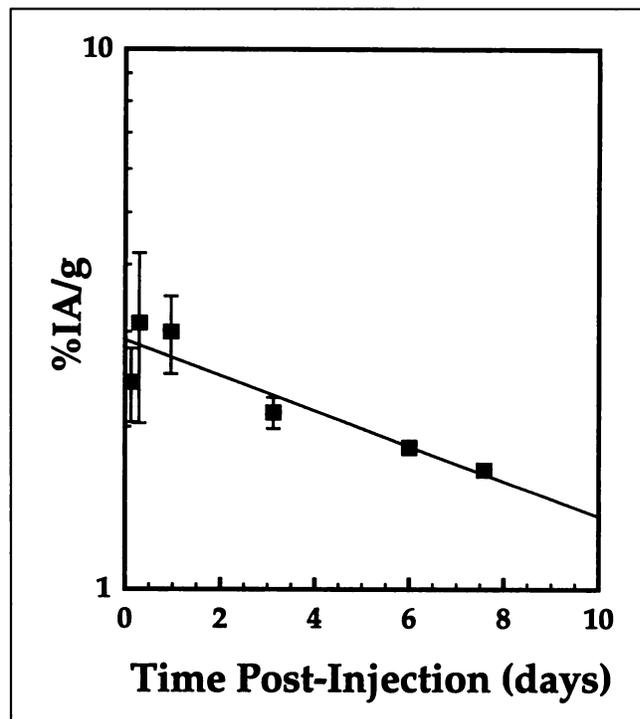

FIGURE 2. Effective clearance of radioactivity from muscle surrounding femurs of mice after intravenous administration of ^{32}P-orthophosphate. Percent injected activity per gram muscle (%IA/g) is given for 1 experiment. Results indicate that muscle takes up ^{32}P quickly and subsequently clears it with effective half-time of about 9.4 d.
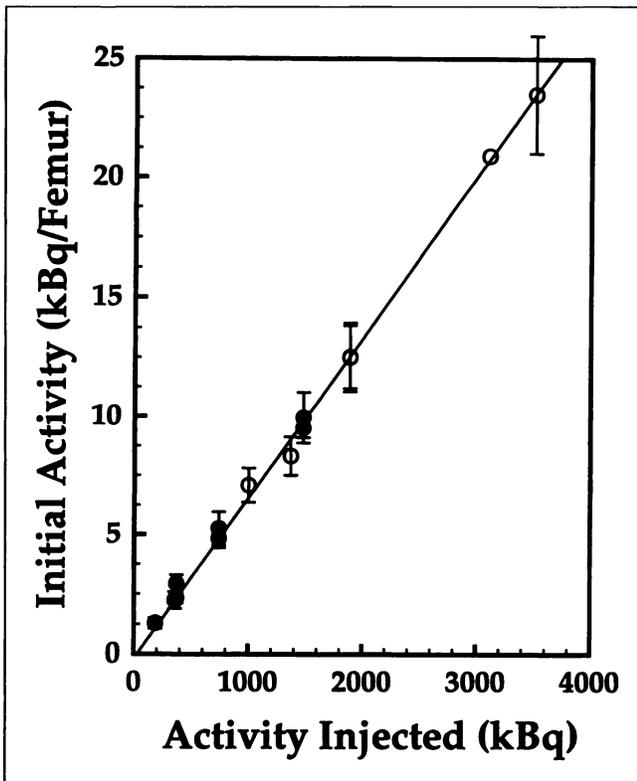
FIGURE 3. Uptake of radioactivity in femoral bone as function of injected activity after intravenous administration of ^{32}P-orthophosphate (●) and ^{33}P-orthophosphate (○). Uptake is linearly proportional to injected activity. Data represent mean of 3 independent experiments. SDs are indicated by error bars.

injected activities ($A_{Inj,37}$) required to achieve 37% survival were used to determine the dose received by the femoral marrow per unit injected activity (D/A_{Inj}). These values are given in Tables 1 and 2.

Bone Measurements

The average femoral marrow and bone masses were 0.0140 ± 0.00464 g and 0.022 ± 0.00155 g, respectively. The average mass of the muscle around the femur was 0.40 ± 0.05 g and the average length of the bone shaft was 10 ± 0.5 mm. This information was used to construct our preliminary femur model for theoretical bone marrow dosimetry.

Theoretical Dosimetry Model

In principle, the absorbed dose to the relevant target regions of the mouse femur (marrow, bone matrix, endosteum) comes from several main sources: (a) activity in the marrow, (b) activity in the bone matrix or on its surface (endosteum), (c) activity in the tissue surrounding the femur, and (d) activity in the remainder of the body. Recently Hui et al. (21) indicated that for pure energetic β-emitters (e.g., ^{90}Y, ^{32}P, ^{33}P), the fourth source is not important. Therefore, the following source activity compartments are considered: endosteum, bone matrix, bone marrow, and muscle surrounding the femur.

For these theoretical femur dosimetry calculations, a simple cylindric geometry was based on the femur mass and dimensions determined using the procedures given in the Material and Methods section of this article. The femur is
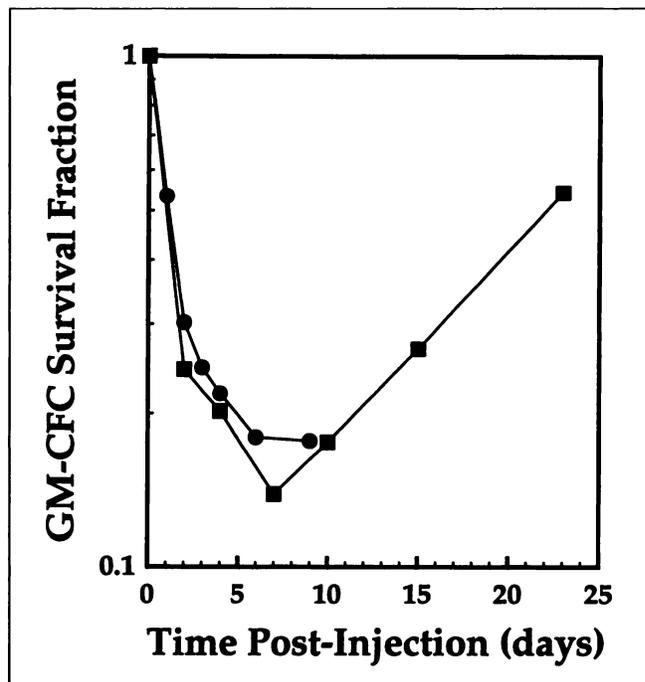
were 313 kBq (8.5 μCi) and 2820 kBq (76 μCi) for ^{32}P and ^{33}P, respectively (Table 1).

Calibration of the Biologic Dosimeter

The survival of GM-CFC as a function of initial dose rate (cGy/h) delivered by the ^{137}Cs irradiator is shown in Figure 6 for different T_ds. Three different T_ds (62, 255, and 425 h) were used in these experiments. The data were least-squares fitted to a simple exponential relationship:

$$SF = exp(-r_o/r_{o,37}), \qquad Eq. 3$$

where r_o is the initial dose rate (cGy/h) and $r_{o,37}$ is the initial dose rate required to achieve 37% GM-CFC survival. The $r_{o,37}$ values obtained for the different T_ds are given in Table 2 along with the value for constant dose-rate irradiation. The T_ds that were preset in the ^{137}Cs irradiator correspond to the effective clearance half-times of ^{90}Y-citrate, ^{32}P-orthophosphate, and ^{114m}In-citrate in the mouse femurs. The rationale for this approach has been discussed previously (17,18). With these data in hand, the $r_{o,37}$ may be interpolated for a T_d of 343 h, the effective clearance half-time of ^{33}P. With an $r_{o,37}$ value of 0.88 cGy/h for T_d = 425 h, and an $r_{o,37}$ value of 0.98 cGy/h for T_d = 255 h, then $r_{o,37}$ (T_d = 343 h) = 0.93 cGy/h. These values and their corresponding SDs are summarized in Table 2.

The experimentally measured initial dose rates ($r_{o,37}$) and

FIGURE 4. Survival of GM-CFCs as function of time after injection of 740 kBq ^{32}P-orthophosphate. Data from 2 independent experiments are provided (●, ■). GM-CFC population experiences rapid decline to nadir on day 7, optimal day to assay GM-CFC for biologic dosimetry of femoral marrow irradiated chronically with incorporated radionuclides (18).
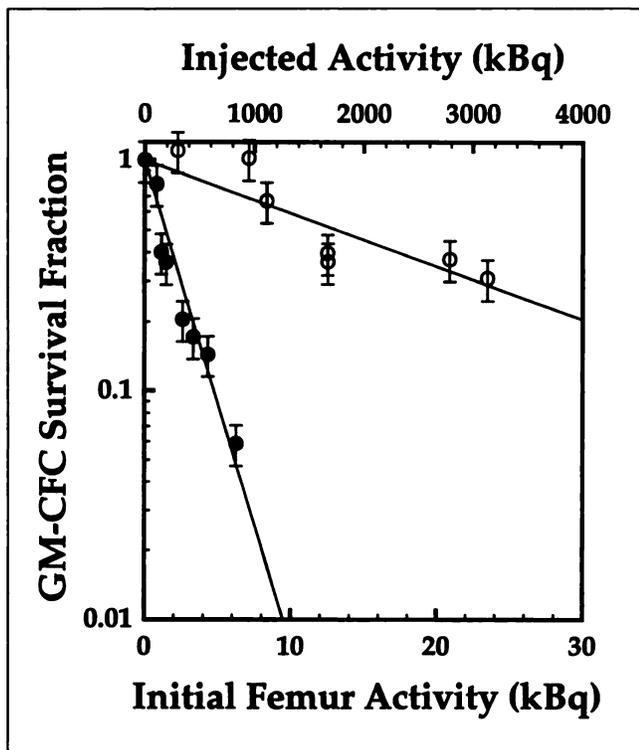
FIGURE 5. Survival of GM-CFCs as function of injected activity and extrapolated initial activity in femoral bone after intravenous administration of ^{32}P-orthophosphate (●) and ^{33}P-orthophosphate (○). Animals were killed on seventh day after injection, optimal day for GM-CFC assay (Fig. 4). SDs of mean for 3 independent experiments are shown.
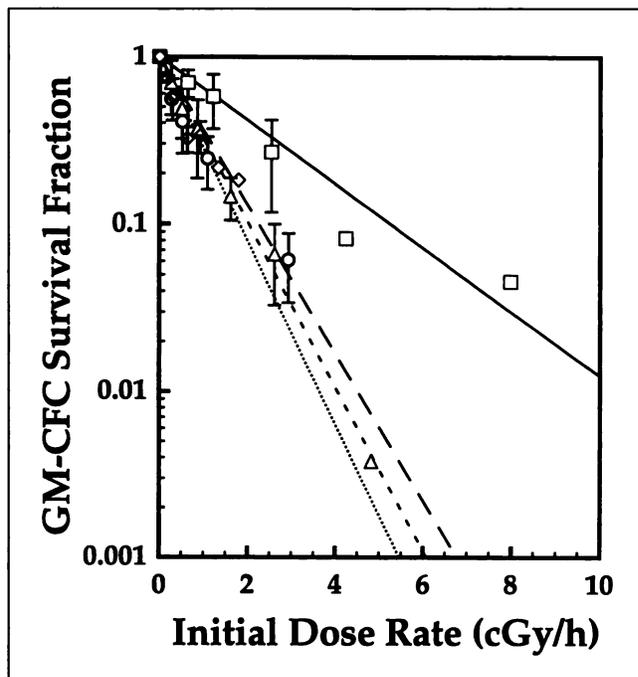

FIGURE 6. Survival of GM-CFCs as function of initial dose rate r_o. Mice were irradiated chronically with exponentially decreasing dose rates of external ^{137}Cs gamma rays (17) and killed on seventh day after initiation of irradiation. Data represent response for 3 different T_ds, including 62 (□, solid line) (18), 255 (○, — —), and 425 h (△, - -), and constant dose rate (◇, dotted line). Data are average of 3 independent experiments with error bars representing SD of mean, and lines are least-squares fits to data.

represented as 3 concentric cylindric annuli (Fig. 7) with a length of 10 mm. The inner cylindric region was considered to be marrow with mass 0.0133 g, density 1.03 g/cm³ (22), and diameter 1.28 mm. The marrow is surrounded by a 10-μm thick annulus of endosteum with mass 0.0004 g and density 1.03 g/cm³ (22). The endosteum is in turn surrounded by a 0.235-mm thick bone annulus with mass 0.022 g and density 1.92 g/cm³ (22). Finally, the bone is covered with a 2.84-mm thick annulus of muscle with mass 0.4 g and density 1.03 g/cm³. In addition to the 4 source regions, 3 target regions are considered including marrow, bone matrix, and endosteum (Fig. 7). A uniform distribution of activity within each source compartment is assumed. The absorbed fractions needed to calculate the mean absorbed

dose to a target region per unit cumulated activity of either ^{32}P or ^{33}P in a source region is calculated using the EGS4 Monte Carlo code (23).

To calculate the absorbed fractions, the cylindric model of the femur is coupled to the electron/photon transport code EGS4 (Electron Gamma Shower Version 4) (23). EGS4 is a general-purpose Monte Carlo code capable of following the coupled transport of photons and electrons within any user-defined geometry and source/target media. We have

TABLE 1
Response of GM-CFC to Injected Radiopharmaceuticals

Radio-pharmaceutical	T_e (h)	$A_{o,37}$ (kBq)	$A_{Inj,37}$ (kBq)	D(marrow)/A_{Inj} (cGy/kBq)
^{90}Y-citrate	62	5.1 ± 0.20	640 ± 25	0.23 ± 0.026
^{32}P-orthophosphate	255	2.1 ± 0.11	313 ± 29	0.42 ± 0.055
^{33}P-orthophosphate	343	18.9 ± 2.3	2820 ± 425	0.047 ± 0.010

T_e = effective clearance half-time of radiopharmaceutical from femoral bone; D(marrow)/A_{Inj} = $D_{37}/A_{Inj,37}$.

TABLE 2
Calibration of Biologic Dosimeter: Response of GM-CFC to Exponentially Decreasing Dose-Rates of ^{137}Cs γ Rays

T_d (h)	$r_{o,37}$ (cGy/h)	D_{37} (cGy)
62*	1.9 ± 0.20	144 ± 15
255	0.98 ± 0.090	132 ± 12
343	0.93 ± 0.14†	132 ± 20
425	0.88 ± 0.019	129 ± 3
∞‡	0.79 ± 0.060	133 ± 10

*Data from reference 18.
†Interpolated from the 255- and 425-h data points.
‡Constant dose rate.
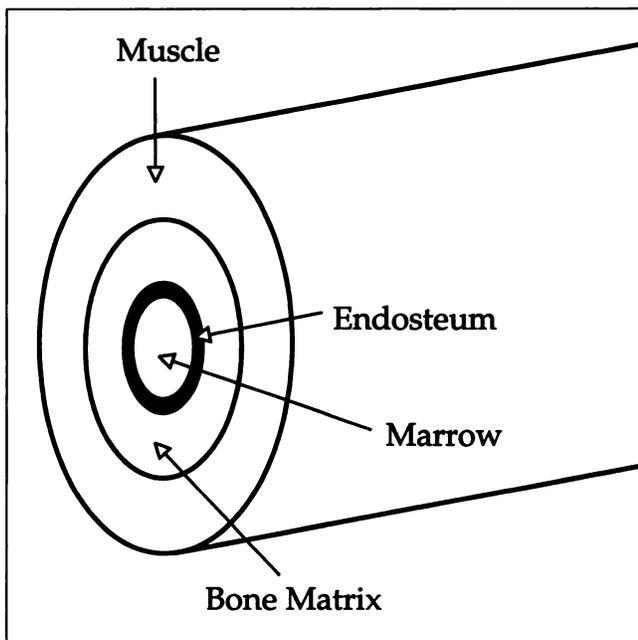D_{37} = absorbed dose required to achieve 37% survival at GM-CFC nadir.

FIGURE 7. Cylindric model of femur from female Swiss Webster mouse, 5–6 wk old.

used this code extensively for performing a variety of internal dosimetry simulation studies (24–28). Because of the small dimensions of the model regions, the PRESTA algorithms of EGS4 were used for all transport simulations.

Within the EGS4 code system, the user assigns atomic composition data for each source region. Standard tissue composition data from the International Commission on Radiation Units and Measurements (22) are used. The slight differences in mouse/human tissue composition for the bone matrix and the bone marrow should not influence the transport simulations. Next, the user randomly assigns a starting location within the source region of interest (e.g., endosteum) for the emission of β particles or low-energy photons. Each particle is followed within the simulation, keeping track of the amount of deposited energy in the target regions. At least 1×10^6 histories were followed, and the fraction of energy emitted in the source that is absorbed in the target (absorbed fraction) was determined. The mean absorbed dose to the target per unit cumulated activity in the source S was then calculated according to S (target ← source) = $\Delta\phi$(target ← source)/m, where ϕ is the absorbed fraction, m is the mass of the target, and Δ is the equilibrium dose constant in kg/Gy/Bqs (30). The values of Δ are taken from the radionuclide data of Eckerman et al. (29).

DISCUSSION

Biokinetics of Radionuclides

Least-squares fits to data in Figure 1 yield effective clearance half-times from the femoral bone of 10.6 ± 1.6 and 14.3 ± 1.6 d for ^{32}P and ^{33}P, respectively. Using these effective half-times and the physical half-lives of these radionuclides [14.26 and 25.4 d, respectively (30)], the

biologic half-times in the femoral bone for ^{32}P- and ^{33}P-orthophosphate are 43 ± 26 and 33 ± 9 d, respectively. Hence, within experimental errors, the biologic clearance half-times are essentially the same for these radionuclides. The large error in the case of ^{32}P is the result of the sensitivity of the error analysis calculation when the physical half-life and effective half-time are similar. These biologic half-times are similar to values obtained for ^{32}P-orthophosphate in human bones (1). As expected, the femoral uptake of ^{32}P- and ^{33}P-orthophosphate show the same linear dependence on injected activity (Fig. 3). Therefore, the uptake and clearance data suggest that these 2 radionuclides follow the same biodistribution patterns in bone. Finally, the data in Figures 1 and 2 show that the effective clearance of ^{32}P from muscle (T_e = 226 h) and bone (T_e = 255 h) is similar.

Optimal Day

Figure 4 shows that the optimal day to kill the animals for the GM-CFC assay is the seventh day after injection of ^{32}P-orthophosphate. These results are similar to those observed for ^{90}Y-citrate (18), ^{117m}Sn-DTPA (unpublished data), and ^{114m}In-citrate (unpublished data), which cleared from the femurs with effective half-times of 62, 223, and 425 h, respectively. However, the cell population recovered more quickly in the animals injected with ^{90}Y-citrate (18). This is likely the result of a more rapid decrease in dose rate delivered by this radiopharmaceutical. In any case, at least for effective half-times ranging from 62 to 425 h, the seventh day after injection is the optimal day to kill animals for a GM-CFC dose–response study. Accordingly, the seventh day after injection was also selected as the kill day for ^{33}P-orthophosphate.

Calibration of GM-CFC as a Biologic Dosimeter for Marrow

Figure 6 and Table 2 indicate that the survival of GM-CFC is dependent both on the initial dose rate r_0 and the effective T_d. The smaller the T_d, the larger the initial dose rate required to achieve equivalent lethal effect. This is because the cumulated dose is an important determinant in dictating the ultimate biologic effect. The cumulated absorbed dose (D) delivered by the irradiator over the 7-d irradiation period is given by:

$$D = r_0 \int_0^{168 \text{ h}} \exp(-0.693t/T_d)\, dt. \qquad \text{Eq. 4}$$

Figure 8 shows the GM-CFC survival as a function of cumulated absorbed dose received by the marrow. Least-squares fits to the data to the function expressed by:

$$SF = \exp(-D/D_{37}), \qquad \text{Eq. 5}$$

yield D_{37} values of 144 ± 15, 132 ± 12, 129 ± 3, and 133 ± 10 cGy for T_ds of 62, 255, 425, and ∞ (constant dose rate), respectively. These experiments involving chronic irradiation of the mice by external beams of ^{137}Cs γ rays with exponentially decreasing dose rates enable examination of
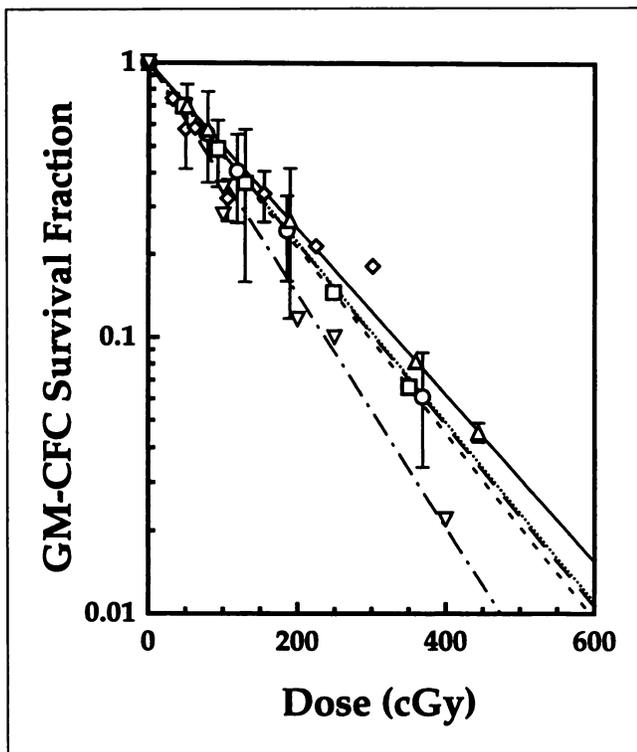
FIGURE 8. GM-CFCs survival as function of cumulated absorbed dose to femur. Cumulated absorbed doses were integrated over period of 7 d (up to day of kill). Data represent dose response for 3 different T_ds, including 62 (□, solid line) (*18*), 255 (○, — —), and 425 h (△, - -), and constant dose rate (◇, dotted line). GM-CFC response to acute external irradiation is also shown (▽, — · —). Data are average of 3 independent experiments with error bars representing SD of mean, and lines are least-squares fits to data.

dose-rate effects in the marrow over the range of T_ds used in this study (62 h $\leq$ Td $<$ ∞). These data suggest that differences in dose rate (0.25–8 cGy/h) among these various T_ds do not play a major role in determining the survival of GM-CFC over the range of initial dose rates, total doses, and irradiation times considered in these experiments with chronic exposures. This finding is in agreement with the data of Wu and Lajtha (*31*). However, the effect of dose rate is clear in the case of acute exposure to [137]Cs γ rays. Figure 8 shows a higher sensitivity of the GM-CFC population to acute exposures with a D_{37} = 103 cGy. It should be noted that in these acute irradiation studies the animals were

irradiated and immediately killed and processed for GM-CFC survival. The D_{37} value of 103 cGy is lower than the average value of 150 cGy reported in Hendry and Lord's (*32*) review of the literature. This difference may be because of our use of murine recombinant granulocyte-macrophage colony-stimulating factor, which was not available at that time.

Experimental Mean Absorbed Dose to Marrow

The mean absorbed dose to murine femoral marrow from ^{32}P and ^{33}P is principally from decays that occur in 3 compartments: femoral marrow, femoral bone matrix, and muscle surrounding the femur. However, in the case of ^{33}P the third component is insignificant, because the low-energy β particles are unable to penetrate through the femoral bone and into the marrow compartment. When properly calibrated, the response of the biologic dosimeter for marrow (GM-CFC survival) registers the cumulative dose from decays that occur in all 3 compartments. Therefore, the experimental mean absorbed dose to bone marrow per unit injected activity $D(marrow)/A_{Inj}$ can be obtained from Equations 2 and 5:

$$D(marrow)/A_{Inj} = D_{37}/A_{Inj,37}. \qquad \text{Eq. 6}$$

These values are summarized in Table 1 for [32/33]P-orthophosphate. The value for ^{90}Y-citrate is provided only as a point of comparison.

Theoretical Mean Absorbed Dose to Bone Marrow (Monte Carlo Calculations)

To estimate the doses received by femoral marrow from internal radionuclides, we have developed a simple theoretical dosimetry model of the mouse femur with 4 source regions (marrow, endosteum, bone matrix, muscle) and 3 target regions (endosteum, bone matrix, bone marrow). This dosimetry model, which is shown in Figure 7 is used to calculate the mean absorbed dose to the target regions in the mouse femur per unit cumulated activity in a given source region of the femur S(target ← source). The resulting theoretical S values are given in Table 3 for the radionuclides ^{32}P and [33]P. The total absorbed dose to the marrow per unit administered activity is given by (*33*):

$$D(marrow)/A_{Inj} = |\tau(bone)\ S(marrow \leftarrow bone\ matrix) +$$

$$\tau(marrow)\ S(marrow \leftarrow marrow) +$$

$$\tau(muscle)\ S(marrow \leftarrow muscle)|, \qquad \text{Eq. 7}$$

TABLE 3
Theoretical S Values (cGy/kBq/h)

| | Target | | | | | |
| | [32]P | | | [33]P | | |
Source	Marrow	Endosteum	Matrix	Marrow	Endosteum	Matrix
Marrow	0.786	0.595	0.338	0.319	0.149	0.0174
Endosteum	0.589	1.22	0.411	0.150	1.61	0.0911
Matrix	0.395	0.484	0.427	0.0202	0.109	0.180
Muscle	0.044	0.0457	0.0449	0.000	0.000	0.001

where τ(source) is the residence time in the source region (*33*):

$$\tau(source) = \tilde{A}(source)/A_{Inj}. \qquad \text{Eq. 8}$$

These quantities are summarized in Table 4 for ^{32}P- and ^{33}P-orthophosphate for each source region, along with the total absorbed dose to the marrow per unit administered activity. Based on the fact that orthophosphate is considered a bone-volume seeker (*34*), it is assumed that the radioactivity in the femoral bone is distributed uniformly in the bone matrix. The calculated D(marrow)/A_{Inj} for ^{32}P-orthophosphate is 0.46 cGy/kBq, which is in good agreement with the experimentally determined 0.42 $\pm$ 0.055 cGy/kBq given in Table 1. In the case of ^{33}P-orthophosphate, the calculated D(marrow)/A_{Inj} value is 0.039 cGy/kBq, which is within the uncertainties of the experimental value of 0.047 $\pm$ 0.01 cGy/kBq. Therefore, our simple theoretical dosimetry model worked reasonably well in predicting the marrow dose. It can be used similarly to predict the absorbed dose received by other target regions in the femur, such as endosteum and bone matrix.

Marrow-Sparing Effects of ^{33}P-Orthophosphate Versus ^{32}P-Orthophosphate for Palliation of Bone Pain

The main limiting factor in radiopharmaceutical therapy for bone pain is bone marrow toxicity. This may be because the high-energy β emitters that are currently in use (e.g., ^{89}Sr, ^{32}P) not only irradiate sites associated with reduction of pain but also the bone marrow. It has been hypothesized that this toxicity can be reduced or eliminated through the use of low-energy (i.e., short-range) β or conversion electron emitters (*13,14,35,36*). An ideal radiopharmaceutical would be one that eliminates the pain without damaging the bone marrow or any other healthy tissue. To compare the relative effectiveness of 2 radionuclides (attached to the same pharmaceutical) for palliation of bone pain, one must be able

to estimate both the absorbed dose to the marrow and the absorbed dose to the target regions that are responsible for the pain relief. Unfortunately, the pathogenesis of alleviation of metastatic bone pain by radiation is poorly understood (*3*). Although a host of different mechanisms have been advanced, none have definitively been established (*37*). Garrett (*38*) reviewed the mechanistic aspects of bone destruction by osteometastases. In this review, it was suggested that the main pathway for bone resorption during this process is through increased osteoclastic activity. Several factors could affect osteoclastic activity. Among them is the fact that many types of tumor cells have been shown to release osteoclastic stimulatory factors. For example, it has been shown that breast cancer cells produce transforming growth factor α, which is a powerful stimulator of osteoclast formation and osteoclastic bone resorption. Cytokine lymphotoxin is another powerful stimulator of osteoclastic bone resorption. These mechanisms suggest that the primary target for relief of bone pain could be regions of high osteoclastic activity (i.e., the tumor–bone interface). It has also been reported that bone itself contains growth factors that may be important for local growth of tumors. Interestingly, Hoskin et al. (*37*) have suggested that the site of action of the palliative therapy may be the interface between normal bone and tumor, or normal bone itself.

In view of the uncertainty in target location for alleviation of bone pain, analyses comparing ^{32}P- and ^{33}P-orthophosphate are performed using either bone matrix or endosteum as the target region. The total absorbed dose to the target per unit injected activity is given by (*33*):

$$D(target)/A_{Inj} = \tau(bone)\ S(target \leftarrow bone\ matrix) +$$

$$\tau(muscle)\ S\ (target \leftarrow muscle) +$$

$$\tau(marrow)\ S(target \leftarrow marrow). \qquad \text{Eq. 9}$$

TABLE 4
Theoretical Absorbed Dose to Marrow from $^{32/33}$P-Orthophosphate

Source	T_e (h)	$A_{o,37}$ (source) (kBq)	$\tilde{A}_{37}$ (source) (kBq/h)*	τ (h)	S (marrow ← source) (cGy/kBq/h)	D(marrow)/A_{Inj} (cGy/kBq)†
^{32}P-orthophosphate						
Bone	255	2.10	283	0.905	0.395‡	0.357
Marrow	255	0.134	18.1	0.0578	0.786	0.045
Muscle	226	3.60	472	1.51	0.0443	0.067
Total						0.469
^{33}P-orthophosphate						
Bone	343	18.9	2703	0.959	0.0202‡	0.0194
Marrow	343	1.21	173	0.0613	0.319	0.0196
Muscle	318	32.4	4550	1.63	0.000	0.00
Total						0.0390

*Cumulated activity is integrated from t = 0 to t = 7 d, the GM-CFC survival nadir.
†Calculated using Equation 9.
‡Assumes radioactivity in bone is localized in bone matrix.

Because the uptake of radioactivity in the bone, muscle, and marrow compartments is rapid, Equation 9 can be approximated by:

$$D(target)/A_{Inj} \approx$$

$$1.44 \, [T_e(bone) \, A_o(bone) \, S(target \leftarrow bone \; matrix) +$$

$$T_e(muscle) \, A_o(muscle) \, S(target \leftarrow muscle) +$$

$$T_e(marrow) \, A_o(marrow) \, S(target \leftarrow marrow)]/A_{Inj}, \quad Eq. \; 10$$

where T_e is the effective half-time of the radioactivity in the source compartment and A_o is the extrapolated initial uptake of activity in the source compartment. These quantities are given in Table 5 for both radionuclides, along with the theoretical mean absorbed dose to the bone matrix and endosteum per unit injected activity of [32]P- and ^{33}P-orthophosphate. These data and those in Table 4 on bone marrow dose can be used to examine the capacity of ^{33}P-orthophosphate to deliver a higher therapeutic absorbed dose to the target than ^{32}P-orthophosphate, for a given deleterious biologic effect on the bone marrow. This can be quantified in terms of a relative advantage factor (RAF), which is given by:

$$RAF = \left[\frac{D(target)}{D(marrow)}\right]_{33P} \Big/ \left[\frac{D(target)}{D(marrow)}\right]_{32P}, \quad Eq. \; 11$$

where ^{33}P serves as the test radiation source and ^{32}P serves as the reference radiation source. When the endosteum is taken as the target region and the bone matrix is taken as the source region for bone activity, there is a 3.2-fold target-dose advantage for the low-energy β emitter [33]P. Similarly, when the bone matrix is taken as the target region and bone matrix is taken as the source region for bone activity, one obtains a 5.6-fold advantage for [33]P. This is in good agreement with the RAF obtained using a theoretical dosimetry model of the

human skeleton when the residence times of [32]P- and ^{33}P-orthophosphate in bone are approximately 15 times higher than in marrow (Table 4) *(36)*. Not accounted for in this analysis for orthophosphate is the high uptake of radioactivity in muscle. This high uptake leads to high absorbed dose to muscle and, therefore, other ^{33}P radiopharmaceuticals may be more appropriate than ^{33}P-orthophosphate for palliation of bone pain *(13,36)*.

Marrow-Sparing Effects of Low-Energy β Emitters Versus High-Energy β Emitters for Palliation of Bone Pain

Our experimental data and analyses thus far have focused on the radiopharmaceuticals [33]P- and ^{32}P-orthophosphate. Other radiopharmaceuticals that target different regions in the bone can be prepared with these radionuclides *(13)*. Accordingly, our experimentally validated theoretical dosimetry model of the mouse femur (Fig. 7) can be used to assess the relative advantage of the low-energy β emitter ^{33}P compared with the high-energy β emitter ^{32}P for other likely target–source geometries. For example, if the endosteum is taken as both the source and target region, a substantially higher RAF will be obtained. However, a substantially lower RAF will be obtained if the endosteum is taken as the source and the bone matrix as the target. These variables are addressed in detail elsewhere *(36)*.

Not accounted for in our analyses is the issue of dose rate to the target region and its impact on pain reduction. Clearly, studies are needed to explore the relationship between dose rate to the target region and reduction of pain. Furthermore, the RAF values discussed in this study are based on experimental measurements and theoretical calculations for normal bone. The uptake of radioactivity is generally much higher in diseased bone *(39)*, thereby leading to an increased local absorbed dose *(7)* with little change in overall marrow

TABLE 5
Theoretical Absorbed Dose to Bone Matrix and Endosteum from [32/33]P-Orthophosphate

Source	T_e (h)	$A_{o,37}$ (source) (kBq)	S (matrix ← source) (cGy/kBq/h)	S (endo ← source) (cGy/kBq/h)	$\dfrac{D(matrix)}{A_{Inj}}$ (cGy/kBq)*†	$\dfrac{D(endo)}{A_{Inj}}$ (cGy/kBq)*†
[32]P-orthophosphate						
Bone‡	255	2.10	0.427	0.484	1.05	1.19
Marrow	255	0.134	0.338	0.595	0.053	0.093
Muscle	226	3.60	0.0449	0.0457	0.168	0.171
Total					1.27	1.45
[33]P-orthophosphate						
Bone‡	343	18.9	0.180	0.109	0.596	0.361
Marrow	343	1.21	0.0174	0.149	0.0037	0.032
Muscle	318	32.4	0.001	0	0.00053	0.00
Total					0.600	0.39

*Calculated using Equation 10.
†Cumulated absorbed dose is integrated from t = 0 to t = ∞.
‡Assumes radioactivity in bone is localized in bone matrix.

dose. Therefore, if the target for alleviation of bone pain is in the immediate vicinity of the metastases, the RAF values would be even higher than those calculated here. Nevertheless, the findings in this study provide strong experimental support for the hypothesis that low-energy β and electron emitters such as ^{33}P and [117m]Sn offer a substantial therapeutic advantage in the palliation of bone pain (14,35).

CONCLUSION

Bone-seeking radionuclides that emit energetic β particles (^{32}P, ^{89}Sr, [186]Re, [153]Sm) have enjoyed considerable success in alleviating bone pain from osseous metastases. However, bone marrow toxicity is frequently a problem that limits both the activity administered as well as the treatment frequency (3,40). The experimental and theoretical approach used in this article supports the hypothesis that low-energy electron or β-particle emitters, such as ^{33}P, offer a substantial therapeutic advantage in that they have the potential to deliver high doses to bone and at the same time minimize the absorbed dose to the bone marrow (12–14,35). More specifically, the data presented in this study suggest that the low-energy β emitter ^{33}P is a better choice for reduction of bone pain. Furthermore, this radionuclide may also be useful in the treatment of bone metastases.

ACKNOWLEDGMENTS

REFERENCES

1. Silberstein EB, Elgazzar AH, Kapilivsky A. Phosphorus-32 radiopharmaceuticals for the treatment of painful osseous metastases. Semin Nucl Med. 1992;22:17–27.
2. Ackery D, Yardley J. Radionuclide-targeted therapy for the management of metastatic bone pain. Semin Oncol. 1993;20(suppl 2):27–31.
3. Lewington VJ. Cancer therapy using bone-seeking isotopes. Phys Med Biol. 1996;41:2027–2042.
4. Friedell HL, Storaasli JP. The use of radioactive phosphorus in the treatment of carcinoma of the breast with widespread metastases to the bone. AJR. 1950;64:559–575.
5. Robinson RG, Preston DF, Schiefelbein M, Baxter KG. Strontium 89 therapy for the palliation of pain due to osseus metastases. JAMA. 1995;274:420–424.
6. de Klerk JMH, van het Schip AD, Zonnenberg BA, et al. Phase 1 study of rhenium-186-HEDP in patients with bone metastases originating from breast cancer. J Nucl Med. 1996;37:244–249.
7. Samaratunga RC, Thomas SR, Hinnefeld JD, et al. A Monte Carlo simulation model for radiation dose to metastatic skeletal tumor from rhenium-186(Sn)-HEDP. J Nucl Med. 1995;36:336–350.
8. Alberts AS, Brighton SW, Kempff P, et al. Samarium-153-EDTMP for palliation of ankylosing spondylitis, Paget's disease, and rheumatoid arthritis. J Nucl Med. 1995;36:1417–1420.
9. Collins C, Eary JF, Donaldson G, et al. Samarium-153-EDTMP in bone metastases of hormone refractory prostate carcinoma: a phase I/II trial. J Nucl Med. 1993;34:1839–1844.
10. Hosain F, Spencer RP. Radiopharmaceuticals for palliation of metastatic osseous lesions: biologic and physical background. Semin Nucl Med. 1992;22:11–16.
11. Kaplan E, Miree J Jr, Hirsh E, Field T. Autoradiographic localization of ^{32}P phosphate in metastatic carcinoma of the breast to bone. Int J Appl Radiat Isotop. 1959;5:94–98.
12. Potsaid MS, Irwin RJ Jr, Castronovo FP, et al. [^{32}P]Diphosphonate dose determination in patients with bone metastases from prostatic carcinoma. J Nucl Med. 1978;19:98–104.
13. Tofe AJ, Francis MD, Slugh CL, Merritt AK, Harvey WJ. P-33 EHDP and P-32 (EHDP, PPi, and Pi) tissue distributions in considerations of palliative treatment for osseous neoplasms [abstract]. J Nucl Med. 1976;17:548.
14. Atkins HL, Mausner LF, Srivastava SC. Sn-117m(4+)DTPA for palliation of painful osseous metastases. A pilot study. J Nucl Med. 1995;36:725–729.
15. Swailem FM, Krishnamurthy GT, Srivastava SC, et al. In-vivo tissue uptake and retention of Sn-117m(4+)DTPA in a human subject with metastatic bone pain and in normal mice. Nucl Med Biol. 1998;25:279–287.
16. International Commission on Radiation Units and Measurements. Stopping Powers for Electrons and Positrons. Report 37. Bethesda, MD: International Commission on Radiation Units and Measurements; 1984.
17. Howell RW, Goddu SM, Rao DV. Design and performance characteristics of an experimental Cs-137 irradiator to simulate internal radionuclide dose rate patterns. J Nucl Med. 1997;38:727–731.
18. Goddu SM, Howell RW, Giuliani DC, Rao DV. Biological dosimetry of bone marrow for incorporated [90]Y. J Nucl Med. 1998;39:547–551.
19. Testa NG. Clonal assays for haemopoietic and lymphoid cells in vitro. In: Potten CS, Hendry JH, eds. Cell Clones: Manual of Mammalian Cell Techniques. Edinburgh, Scotland: Churchill-Livingstone; 1985:27–43.
20. Metcalf D. Hemopoietic colonies: in vitro cloning of normal and leukemic cells. Recent Results Cancer Res. 1977;61:1–227.
21. Hui TE, Fisher DR, Kuhn JA, et al. A mouse model for calculating cross-organ beta doses from yttrium-90-labeled immunoconjugates. Cancer. 1994;73(suppl): 951–957.
22. International Commission on Radiation Units and Measurements. Photon, Electron, Proton and Neutron Interaction Data for Body Tissues. Report 46. Bethesda, MD: International Commission on Radiation Units and Measurements; 1992.
23. Nelson WR, Hirayama RH. The EGS4 code system. Report 265. Palo Alto, CA: Stanford University; 1985.
24. Bouchet LG, Jokisch DW, Bolch WE. A three-dimensional transport model for determining absorbed fractions of energy for electrons within trabecular bone. J Nucl Med. 1999;40:1947–1966.
25. Bouchet LG, Bolch WE. A three-dimensional transport model for determining absorbed fractions of energy for electrons within cortical bone. J Nucl Med. 1999;40:2115–2124.
26. Bouchet LG, Bolch WE. Five pediatric head and brain mathematical models for use in internal dosimetry. J Nucl Med. 1999;40:1327–1336.
27. Bouchet LG, Bolch WE, Weber DA, Atkins HL, Poston JW Sr. MIRD pamphlet no. 15: radionuclide S values in a revised dosimetric model of the adult head and brain. J Nucl Med. 1999;40:62S–101S.
28. Bolch WE, Bouchet LG, Robertson JS, et al. MIRD pamphlet no. 17: the dosimetry of nonuniform activity distributions—radionuclide S values at the voxel level. J Nucl Med. 1999;40:11S–36S.
29. Eckerman KF, Westfall RJ, Ryman JC, Cristy M. Nuclear Decay Data Files of the Dosimetry Research Group. ORNL/TM-12350. Oak Ridge, TN: Oak Ridge National Laboratory; 1993.
30. Weber DA, Eckerman KF, Dillman LT, Ryman JC. MIRD: Radionuclide Data and Decay Schemes. New York, NY: Society of Nuclear Medicine; 1989.
31. Chu-Tse W, Lajtha LG. Haemopoietic stem-cell kinetics during continuous irradiation. Int J Radiat Biol Relat Stud Phys Chem Med. 1975;27:41–50.
32. Hendry JH, Lord BI. The analysis of early and late response to cytotoxic insults in the haematopoietic cell hierarchy. In: Potten CS, Hendry JH, eds. Cytotoxic Insult to Tissue. Edinburgh, Scotland: Churchill-Livingstone; 1983:1–66.
33. Loevinger R, Budinger TF, Watson EE. MIRD Primer for Absorbed Dose Calculations. Revised. New York, NY: The Society of Nuclear Medicine; 1991.
34. Spiers FW, Beddoe AH, Whitwell JR. Mean skeletal dose factors for beta-particle emitters in human bone. Part I: volume-seeking radionuclides. Br J Radiol. 1978;51:622–627.
35. Krishnamurthy GT, Swailem FM, Srivastava SC, et al. Sn-117m(4+)DTPA pharmacokinetics and imaging characteristics in patients with metastatic bone pain. J Nucl Med. 1997;38:230–237.
36. Bouchet LG, Bolch WE, Goddu SM, Howell RW, Rao DV. Considerations in the selection of radiopharmaceuticals for palliation of bone pain from metastatic osseous lesions. J Nucl Med. 2000;41:682–687.
37. Hoskin PJ, Ford HT, Harmer CL. Hemibody irradiation for metastatic bone pain in two histologically distinct groups of patients. 1989;1:67–69.
38. Garrett IR. Bone destruction in cancer. Semin Oncol. 1993;20:4–9.
39. Silberstein EB. The treatment of painful osseus metastases with phosphorus-32-labeled phosphates. Semin Oncol. 1993;20(suppl 2):10–21.
40. Silberstein EB. Dosage and response in radiopharmaceutical therapy of painful osseus metastases. J Nucl Med. 1996;37:249–252.